Cavity ringdown spectrum of the forbidden $\tilde{A}^2E'' \leftarrow \tilde{X}^2A_2'$ transition of NO_3: Evidence for static Jahn–Teller distortion in the $\tilde{A}$ state

Andrei Deev, Jonas Sommar,[a] and Mitchio Okumura[b]
Arthur Amos Noyes Laboratory of Chemical Physics, California Institute of Technology, Pasadena, California 91125

(Received 10 January 2005; accepted 3 March 2005; published online 13 June 2005)

The Jahn–Teller effect in the first two excited states of the nitrate radical NO_3 has yet to be experimentally elucidated. In this paper, direct evidence of strong Jahn–Teller interactions in the $\tilde{A}$ state is presented from the first complete absorption spectrum of the $\tilde{A}^2E'' \leftarrow \tilde{X}^2A_2'$ transition of NO_3 in the gas phase in the region 5900–9000 cm^{-1}, at moderate resolution (0.15 cm^{-1}). The observed spectrum is consistent with Herzberg–Teller selection rules, and reveals strong linear and quadratic Jahn–Teller interactions in the $\tilde{A}$ state. Several of the vibronic bands have been tentatively assigned, including ν_2, ν_3, an irregular progression in ν_4, and combination bands involving ν_1. Our assignments are consistent with the previous works of Weaver *et al.* [A. Weaver, D. W. Arnold, S. E. Bradforth, and D. M. Neumark, J. Chem. Phys. **94**, 1740 (1991)] and Hirota *et al.* [E. Hirota, T. Ishiwata, K. Kawaguchi, M. Fujitake, N. Ohashi, and I. Tanaka, J. Phys. Chem. **107**, 2829 (1997)] The band origin is not observed, in accord with the selection rules, but is determined to be $T_0 = 7064$ cm^{-1} from the observation of the 4_1^0 hot band at 6695.7 cm^{-1}. Rotational contour analysis of this band indicates that the upper state is an asymmetric rotor, establishing that NO_3 undergoes static Jahn–Teller distortion in the ground vibrational level of the $\tilde{A}$ state. © *2005 American Institute of Physics*. [DOI: 10.1063/1.1897364]

I. INTRODUCTION

As an open-shell molecule with D_{3h} symmetry, the nitrate radical NO_3 exhibits the Jahn–Teller effect in its degenerate electronic states. There have been many detailed theoretical studies of the vibronic interactions in the ground and the first two excited states of NO_3, and this radical has become a model system for studying the Jahn–Teller and pseudo-Jahn–Teller effects. However, despite numerous spectroscopic studies, there is little direct experimental data on the Jahn–Teller effect in gas phase NO_3.

Walsh[1] correctly predicted the electronic configuration of the ground state, $(4e')^4(1e'')^4(1a_2')^1$, and proposed that the three orbitals were all close in energy. Single excitations from the $(1e'')$ and $(4e')$ orbitals to the $(1a_2')$ orbital produce the first two excited states, $\tilde{A}^2E''$ and $\tilde{B}^2E'$, respectively. The geometry of the ground $\tilde{X}^2A_2'$ state was the subject of some controversy, and only recently have experiment and theory confirmed that it has a planar D_{3h} geometry.[2–7] The two excited states must exhibit the Jahn–Teller effect, but neither excited state is well characterized. A quantitative description of the Jahn–Teller effect in NO_3 is complicated because all three levels interact via vibronic coupling,[8] and NO_3 has two Jahn–Teller active modes, the degenerate asymmetric stretch ν_3 and bend ν_4 vibrations, rendering it a multimode problem.

The higher $\tilde{B} \leftarrow \tilde{X}$ transition, first observed in the gas phase by Jones and Wulf,[9] gives rise to broad, relatively unstructured absorption bands between 680 and 450 nm. The transition is strong [σ (662 nm) $= 2.2 \times 10^{-17}$ cm^2] and has been studied extensively,[10–12] but the upper vibronic levels have only been tentatively assigned,[13] and even jet cooling has not helped.[14] The spectral complexity, line broadening, and anomalous fluorescence decay all suggest strong vibronic coupling.

There have been few experimental studies of the first electronic state $\tilde{A}^2E''$ of NO_3. The transition $\tilde{A} \leftarrow \tilde{X}$ is forbidden, but it is vibronically allowed by the Herzberg–Teller effect and therefore weak. Weaver *et al.*[5] first observed the $\tilde{A}$ state by anion photoelectron spectroscopy (PES) of NO_3^- and found $T_0(\tilde{A}) = 7000 \pm 110$ cm^{-1}. They observed a series of peaks which they fit to mixed progressions of two harmonic modes, 541 ± 8 and 804 ± 4 cm^{-1}. They tentatively assigned these modes to ν_4 and ν_1, respectively. In a Fourier transform infrared (FTIR) spectrum of NO_3,[15] Kawaguchi *et al.* discovered two near infrared (NIR) absorption bands at 7602 and 7744 cm^{-1}, which they assigned to the 4_0^1 and 2_0^1 transitions, though only band positions and type were listed. Hirota *et al.* employed diode laser spectroscopy to obtain a rotationally resolved spectrum of the 7602-cm^{-1} band.[16] They fit the spectrum to a parallel band of a D_{3h} symmetric top, and assigned it to a transition to the $^2A_1''$ vibronic component of the ν_4 mode of the $^2E''$ state. The upper state could be described with a symmetric-top Hamiltonian with a diagonal spin-rotation term, with few perturbations. These results sug-

[a]Department of Chemistry, University of Gothenburg (Göteborg University), 412 96 Gothenburg (Göteborg), Sweden.
[b]Author to whom correspondence should be addressed; electronic mail: mo@caltech.edu

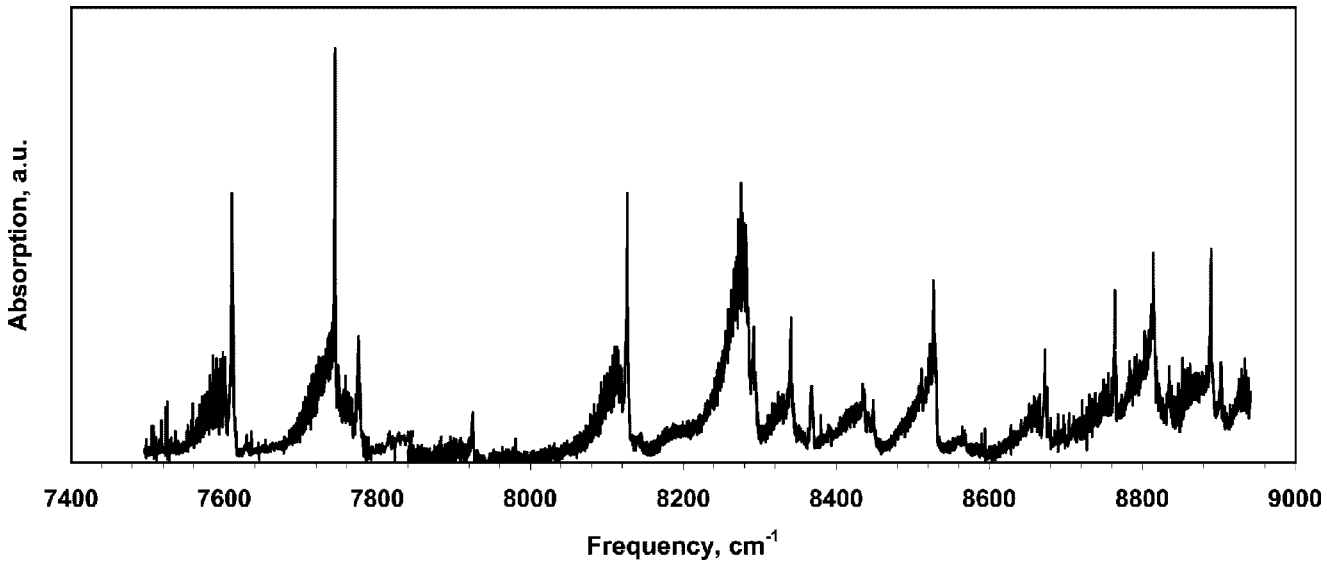

FIG. 1. Cavity ringdown spectrum of the $\tilde{A}^2E'' \leftarrow \tilde{X}^2A_2'$ transition of NO_3. The origin is estimated to be $\nu_0 = 7064\ cm^{-1}$.

gest that NO_3 in the $\tilde{A}$ state is symmetric, i.e., it exhibits the dynamic Jahn–Teller effect with weak vibronic interactions.

This result appears to disagree with a high-level *ab initio* study of the excited states of NO_3 by Eisfeld and Morokuma.[17] They optimized the structures of NO_3 in the $\tilde{A}$ and $\tilde{B}$ states at the complete active space self-consistent field (CASSCF) and multi-reference single and double excitation configuration interaction (MR-SDCI) levels of theory. They found that the $\tilde{A}$ state undergoes significant Jahn–Teller distortion. NO_3 in the $\tilde{A}$ state is localized in three C_{2v} minima with B_2 symmetry lying $\approx$2000 cm^{-1} below the conical intersection. The transition states between the minima were 800–1000 cm^{-1} higher in energy. Such a large stabilization energy and high barrier to pseudorotation indicate strong linear and quadratic Jahn–Teller effects in the $\tilde{A}$ state.

Our experimental knowledge of the $\tilde{A}$ state is thus incomplete and at odds with theoretical predictions. Furthermore, the experimental results to date shed little light on the Jahn–Teller effect in NO_3. Barckholtz and Miller[18] have stressed that analyses of single bands are insufficient in describing the Jahn–Teller states, due to the large and erratic variations in band spacings and even rotational structure arising from the vibronic perturbations. Rather, the full spectrum must be acquired and, even then, great care must be taken in assigning vibronic bands. For NO_3, a comprehensive absorption spectrum of the $\tilde{A}$ state can provide definitive insights into the nature of the Jahn–Teller effect in this important molecule.

In this work, we exploit the sensitivity of the cavity ringdown method to detect the forbidden $\tilde{A}^2E'' \leftarrow \tilde{X}^2A_2'$ transition of NO_3 in the range of 5900–9000 cm^{-1}.

II. EXPERIMENT

The NIR absorption spectrum of NO_3 was recorded by pulsed cavity ringdown spectroscopy of room-temperature NO_3 in a flow cell in an apparatus similar to the one used by Pushkarsky *et al.*[19] Tunable NIR radiation was generated by stimulated Raman scattering in hydrogen. The output of a YAG-pumped dye laser (Continuum TDL51 and NY60) was directed through a 2-m-long multipass Raman cell[20] containing 6–9 atm of H_2. The NIR pulse (0.5–1 mJ) was generated as the second Stokes of the dye beam (5–20 mJ, $\approx$0.15 cm^{-1} linewidth) in three passes, and then filtered and slightly focused into the ringdown cell.

Reactant gases were flowed through a 40-cm-long, 1.27-cm-diameter Pyrex cell. Two high reflectivity mirrors formed the optical cavity, which was coaxial with the gas cell, and were separated from the reaction region by 20-cm-long purge volumes. Three sets of mirrors were used: Newport 1-m-ROC (radius of curvature) mirrors (5900–7000 and 7000–8000 cm^{-1}) and Los Gatos Research 6-m-ROC mirrors (7900–8950 cm^{-1}).

The NIR radiation exiting the cavity was tightly focused onto a 1-mm-diameter extended InGaAs photodiode (Hamamatsu). The photodiode signal was amplified and digitized by a 12-bit transient digitizer (Gage Compuscope 1012). Twenty ringdown traces were typically averaged and then fit to a single-exponential function using the NL2SOL algorithm.[21]

NO_3 was produced in a reaction of ozone with N_2O_5. A 1% mixture of O_3 in O_2 passed through a trap containing solid N_2O_5 held at $-20\ ^\circ C$, and was then flowed into the reaction cell. Nitrogen was flowed through the purge volumes to protect the mirrors. The gas in the cell, at a pressure of 45–50 Torr, was flowed through at a rate of 45 sccm (sccm denotes cubic centimeter per minute at STP) (4.5-s residence time). To eliminate absorption by N_2O_5 and residual water, a background scan was taken with the ozonizer off after every run and subtracted from the spectrum. NO_3 was also produced by photolysis of $ClONO_2$ and N_2O_5, to confirm the identity of the observed bands.

The NO_3 concentration was measured between scans by direct absorption at 661.5 nm using a diode laser. The diode laser beam was collinear with the NIR radiation and

detected with the same photodiode. Single pass absorbances were typically 5%–10%, yielding $NO_3 \approx 8\times10^{13}$–$2\times10^{14}$ mol/cm^3.

III. RESULTS

The spectrum of NO_3 is shown in Fig. 1. Scans with different laser dyes were scaled by matching the intensities of the bands present in overlapping regions, or by scaling with the measured NO_3 concentration. We detected a series of absorption bands in the 5900–9000 cm^{-1} range, though absorption by nitric acid prevented the detection between 6900 and 7000 cm^{-1}. Using chemistry, background subtraction, and contour analysis, we attributed all of these bands to NO_3. Only three weak bands were found between 5900 and 7500 cm^{-1}, peaked near 6700 and 7230 cm^{-1}. Above 7500 cm^{-1}, we observed a series of bands (including the two bands reported previously) which became increasingly congested, especially above 8700 cm^{-1}. There are no obvious spin-orbit doublets, indicating that spin-orbit coupling must be largely quenched.

Most of the vibronic bands had sharp *R*-branch bandheads and widths of ≈50 cm^{-1}, though some band shapes were obscured in the congested regions. Simulations of rotational contours with the NO_3 constants obtained by Hirota *et al.* show that parallel and perpendicular bands are easily distinguished: both have sharp *R*-branch bandheads, but perpendicular bands have a sharper bandhead and no gap between the *P* and *R* branches. The majority of the well-resolved bands are perpendicular bands, but five are clearly parallel bands; only the 8287(3)-cm^{-1} band does not resemble the simulated contours. Band centers are estimated from the contour analysis.

IV. ANALYSIS

The forbidden $\tilde{A}\leftarrow\tilde{X}$ transition becomes allowed via vibronic coupling. Only vibronic states with symmetries of $\Gamma_{ve}=A_1''$ or E', for parallel and perpendicular bands, respectively, can be excited by transitions from the 0_0 state. The umbrella mode ν_2 and its odd quanta have $\Gamma_{ve}=a_2''\otimes E''=E'$ symmetry and will give rise to perpendicular bands. The degenerate e' modes ν_3 and ν_4 split into three vibronic states $e'\otimes E''=A_1''\oplus A_2''\oplus E''$ by vibronic coupling. Only the A_1'' component will be observed, as a parallel band, in the absence of spin-orbit coupling. The overtones and combination bands of these modes will split into a larger number of vibronic states of the same symmetries; most components will be forbidden. The symmetric stretch ν_1 is not allowed, and can be observed only in combination with other allowed modes.

The ν_3 and ν_4 modes are Jahn–Teller active and even small Jahn–Teller coupling can split the vibronic levels and lead to irregular spacings.[18] For these modes, v is no longer a good quantum number and is used here to indicate the state with the largest contribution to the eigenfunction of the Jahn–Teller Hamiltonian. The non-Jahn–Teller active modes, however, should behave normally and form regular progressions. Perturbations due to the Jahn–Teller effect make assignments tenuous; in this paper, we therefore assign only the more prominent features.

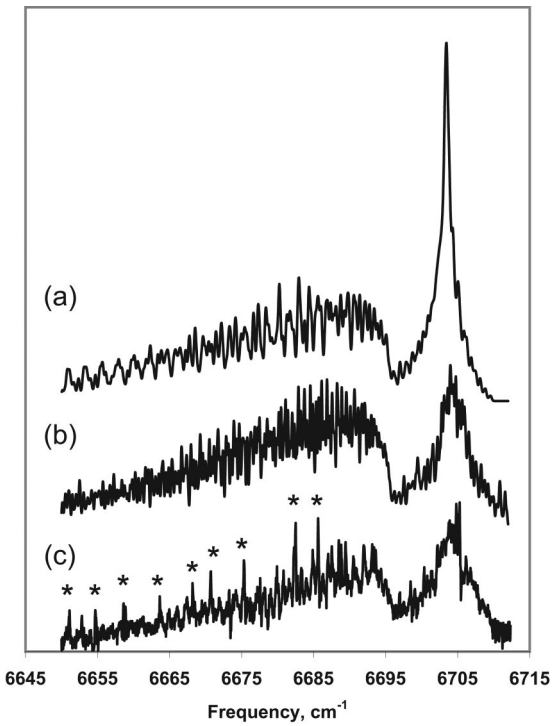

FIG. 2. Spectrum of the 4_1^0 hot band. (a) Simulation-symmetric top, (b) simulation-asymmetric top, and (c) experiment. The * represent positions of strong water lines which may give residual peaks even after background subtraction.

The 0_0^0 band is vibronically forbidden, though a weak absorption was indeed detected between 7040 and 7080 cm^{-1} near the expected origin, $\nu_0 \approx 7060$ cm^{-1}. However, due to the low signal-to-noise ratio (S/N≈10) and interference of the water lines, we could not assign this band unambiguously. A weak parallel transition was observed at 6695.7 cm^{-1} (Fig. 2), ≈365 cm^{-1} below the expected origin. The ν_4'' mode in the ground state is 368 cm^{-1} from laser-induced fluorescence (LIF) measurements,[12] and has a 298-K Boltzmann factor of 0.34, consistent with the observed intensity. We therefore assign this band to the 4_1^0 hot band transition.

This hot band allows us to determine with more confidence the position of the origin. We estimate $T_0(\tilde{A})$ =7064 cm^{-1}. The accuracy is limited by the uncertainty in determining the origin of the LIF band, but this is not known. However, the current value is certainly more accurate than the previously reported value of 7061±8 cm^{-1}, which was based on the ν_4 frequency of 540 cm^{-1} in the PES spectrum. The ±8 cm^{-1} uncertainty comes from fitting the PES peaks to the harmonic progressions.[5] The actual uncertainty in the previous value is likely to be much larger, because the overtone and combination band frequencies of a Jahn–Teller active mode will result in shifts of tens of wavenumbers.

We assign a series of similar parallel bands at 7602(1), 8121(1), and 8668(1) cm^{-1} to a progression in ν_4. Specifically, these are the $|j=3/2,a_1''\rangle$ states of the $n\nu_4 e'\otimes E''$ vibronic manifolds. Here j is a first order Jahn–Teller quantum

number.[18] This confirms the assignment of the 7602.545-cm^{-1} band by Hirota *et al.* The irregular spacings, 539, 519(1), and 547(1) cm^{-1}, are evidence of the Jahn–Teller coupling. While it is conceivable that the weak band at 7230 cm^{-1} could be 4_0^1, its intensity and band shape differ from the others in the progression.

The 7742(1)-cm^{-1} band is the first and strongest of a series of perpendicular bands. Perpendicular bands must involve the umbrella mode, ν_2. The prominence of these bands is expected, because this mode is responsible for the intensity borrowing by pseudo-Jahn–Teller coupling from the strong $\tilde{B} \leftarrow \tilde{X}$ transition. We assign the 7742-cm^{-1} band to the fundamental of ν_2, in agreement with the study of Kawaguchi *et al.*,[15] giving $\nu_2 = 678$ cm^{-1} in the upper state.

The other perpendicular bands are combination bands with ν_2 or its overtones with odd υ_2. The strong perpendicular band at 8527-cm^{-1} band lies 785 cm^{-1} to the blue, which is close to the predicted[17] frequency for the symmetric stretch, $\nu_1 \approx 800$ cm^{-1}. We assign it to the $\nu_1 + \nu_2$ combination band. This value falls between the frequency of the first peak (750 cm^{-1}) in the anion PES spectrum[5] and the (less reliable) value of 804 cm^{-1} obtained from the harmonic fit of the ν_1 progression.

Other possible combination bands with ν_1 include the 8365(3)- and 8900(3)-cm^{-1} bands, which we tentatively assign to $1_0^1 4_0^1$ and $1_0^1 4_0^2$. These bands overlap with adjacent bands, partially obscuring their contours. The values of ν_1 in these combination bands would be 763(3) and 779(3) cm^{-1}, respectively. The differences in apparent ν_1 frequencies are likely due to the intrinsic vibrational anharmonicity and/or to the bilinear vibronic coupling between the ν_1 and ν_4 modes.

We simulated the rotational contours of several vibronic bands in detail to find evidence of the static Jahn–Teller distortion in NO_3. Static distortion leads to the asymmetry in the averaged structure. We employed SPCAT (Ref. 22) and ASYROT (Ref. 23) programs to model the rotational contours using symmetric- and asymmetric-top Hamiltonians, respectively. Our simulations included the known centrifugal constants for the ground state 0_0 and the 4^1 state, but ignored spin-rotation and Coriolis couplings. Because the rotational constants of the 4_1 state are not known, we used the ground 0_0 state constants for the lower state of the 6696-cm^{-1} band (we explicitly assume that the structure retains D_{3h} symmetry in the hot lower level, i.e., with one quantum in ν_4 of the $\tilde{X}$ state).

The observed profiles of the bands in the $n\nu_4$ progression were simulated well using the symmetric top Hamiltonian with the rotational constants of Hirota *et al.*[16] For the 4_0^2 and 4_0^3 bands, the upper-state constants had to be scaled by 0.987 and 0.975, to achieve better agreement, indicating an overall increase in the structure in these levels.

The symmetric-top model, however, failed for the 4_1^0 hot band and the 2_0^1 band. The results of the simulations using both symmetric- and asymmetric-top Hamiltonians for the 4_1^0 band are shown in Fig. 2. The symmetric-top model was not able to predict the width of the bandhead of the 4_1^0 band nor the blue shoulder of the 2_0^1 band. Varying the rotational constant B' of the upper state with locked planar symmetric-top relationship $A' = B' \approx C'/2$ only slightly shifted the position of the bandhead without affecting the overall shape of the band. We found that it was necessary to break the $A' = B'$ symmetry to obtain qualitative agreement with the experiment. The experimental contours of the 4_1^0 and 2_0^1 bands were best simulated with the asymmetric-top Hamiltonian, as a *c*-type($\parallel$) band with $\kappa' = 0.59$ and as a *b*-type($\perp$) band with $\kappa' = 0.83$, respectively.

The strongest band, at 8287(3) cm^{-1}, has an unusual contour that can be simulated only if $\kappa' = 0.32$, i.e., the upper-state geometry is more distorted than in the 0^0 state. The band is a *c*-type($\parallel$) transition and we tentatively assign it to 3_0^1, yielding $\nu_3' = 1223$ cm^{-1}. This assignment must be considered tenuous, given the anomalous band shape and large discrepancy of the band position with theoretical predictions.

V. DISCUSSION

We find clear evidence of a relatively strong Jahn–Teller effect in the $\tilde{A}$ state of NO_3. The 0^0 level undergoes static Jahn–Teller distortion, as do the vibrationally nondegenerate 2^1 and its combination levels. Both of the Jahn–Teller active modes, ν_3 and ν_4, appear to be highly perturbed. The absence of apparent spin-orbit doublets is also indicative of relatively strong linear and quadratic Jahn–Teller couplings, which would largely quench spin-orbit coupling (<150 cm−1).

Previous experimental and theoretical results give a fragmentary and somewhat contradictory picture of the Jahn–Teller effect in the $\tilde{A}$ state of NO_3. Our results are consistent with these earlier studies, but provide a more complete picture and resolve the apparent discrepancy between theory and experiment.

The current results agree with predictions of a strong Jahn–Teller effect by Eisfeld and Morokuma[17] and by Stanton.[24] The observation of a distorted structure for the vibrationally nondegenerate levels of the $\tilde{A}$ state supports the *ab initio* results of Eisfeld and Morokuma and of Stanton. In MR-SDCI calculations, Eisfeld and Morokuma[17] predicted a distorted C_{2v} geometry in a state of $^2B_1$ symmetry with $\kappa = 0.88$. The vibrational frequencies observed for the nondegenerate modes agree fairly well with the MR-SDCI harmonic values ($\nu_1 = 731$ cm^{-1} and $\nu_2 = 802$ cm^{-1}), but those of the degenerate Jahn–Teller active modes deviate significantly from predictions [$\nu_3(b_2) = 1754$ cm^{-1} and $\nu_4(b_2) = 271$ cm^{-1}]. Surprisingly, the state-averaged CASSCF frequencies (800, 684, 1602, and 553 cm^{-1}) are closer for all but ν_3. Stanton's equation of motion ionization potential-coupled cluster with singles and doubles and perturbative triples/triple zeta basis set with double polarization functions (EOMIP-CCSD(T)/TZ2P) calculation[24] predicts a similar distorted $\tilde{A}$ state minimum; the predicted frequencies for $\nu_3(b_2)$ and $\nu_4(b_2)$, are 1570 and 588 cm^{-1}, respectively, in better agreement with experiment.

However, our results also confirm the findings of Hirota *et al.* whose full rotational analysis demonstrated that the a_1'' state of 4^1 has a symmetric D_{3h} structure. We conclude that

the barrier for pseudorotation must lie at or below the 4^1 vibronic level, $E<800$–$1000\ \mathrm{cm}^{-1}$.

The behavior of the ν_3 mode is at first glance puzzling. In the independent mode approximation, the symmetric structure of the ν_4 band would suggest that ν_3 has a small linear Jahn–Teller effect. The asymmetry in the 3^1 state would result because it remains distorted in the Q_4 coordinate space even after excitation of ν_3. However, the 3_0^1 band appears $>300\ \mathrm{cm}^{-1}$ away from *ab initio* predictions, the only mode to deviate so significantly. The increased distortion seen in the 3^1 level indicates that vibrational excitation in ν_3 inhibits pseudorotation. These observations suggest that ν_3 is, in fact, more strongly coupled, not less. These results may be an indication of higher-order coupling of the Jahn–Teller active modes. Indeed, the predicted saddle point for pseudorotation, of $^2A_2$ symmetry in the C_{2v} point group,[17] is distorted along Q_3 and Q_4, as well as Q_1, suggesting that all three modes are coupled and that the independent mode approximation fails. The increased distortion suggests a dynamical localization, with barrier crossing inhibited upon excitation of ν_3 by the need for vibrational exchange. It may be that the bilinear or higher-order coupling of the symmetric mode ν_1 with the Jahn–Teller active modes must be explicitly included.

A complete quantitative description of the Jahn–Teller effect requires detailed modeling of the observed bands, assisted by *ab initio* estimates of the vibronic coupling terms. Thus, the current assignments must be considered somewhat tentative, given the pitfalls in assigning spectra in the presence of strong vibronic coupling.[18] However, this experiment reveals that a wealth of spectroscopic data waits to be mined, and we expect that the $\tilde{A}$ state of NO_3 will become an important quantitative test of models of the Jahn–Teller effect. A more detailed study, including higher-resolution spectra, new *ab initio* results, and shorter-wavelength scans, is underway.

ACKNOWLEDGMENTS

We acknowledge the support of the NASA UARP Contract No. NAG5-11657, and thank B. J. Drouin for help with software and J. F. Stanton, A. I. Krylov, and T. A. Miller for helpful discussions.

[1] A. D. Walsh, J. Chem. Soc., 2301 (1953).
[2] T. Ishiwata, I. Tanaka, K. Kawaguchi, and E. Hirota, J. Chem. Phys. **82**, 2196 (1985).
[3] R. R. Friedl and S. P. Sander, J. Phys. Chem. **91**, 2721 (1987).
[4] K. Kawaguchi, E. Hirota, T. Ishiwata, and I. Tanaka, J. Chem. Phys. **93**, 951 (1990).
[5] A. Weaver, D. W. Arnold, S. E. Bradforth, and D. M. Neumark, J. Chem. Phys. **94**, 1740 (1991).
[6] U. Kaldor, Chem. Phys. Lett. **185**, 131 (1991).
[7] W. Eisfeld and K. Morokuma, J. Chem. Phys. **113**, 5587 (2000).
[8] M. Mayer, L. S. Cederbaum, and H. Koppel, J. Chem. Phys. **100**, 899 (1994).
[9] E. J. Jones and O. R. Wulf, J. Chem. Phys. **5**, 873 (1937).
[10] T. Ishiwata, I. Fujiwara, Y. Naruge, K. Obi, and I. Tanaka, J. Phys. Chem. **87**, 1349 (1983).
[11] H. H. Nelson, L. Pasternack, and J. R. McDonald, J. Phys. Chem. **87**, 1286 (1983).
[12] B. S. Kim, P. L. Hunter, and H. S. Johnston, J. Chem. Phys. **96**, 4057 (1992).
[13] D. A. Ramsay, in *Proceedings of the Tenth Colloquium Spectroscopicum Internationale*, edited by E. R. Lippencott and M. Margoshes (Spartan Books, Washington, DC., 1963), p. 593.
[14] R. T. Carter, K. F. Schmidt, H. Bitto, and J. R. Huber, Chem. Phys. Lett. **257**, 297 (1996).
[15] K. Kawaguchi, T. Ishiwata, E. Hirota, and I. Tanaka, Chem. Phys. **231**, 193 (1998).
[16] E. Hirota, T. Ishiwata, K. Kawaguchi, M. Fujitake, N. Ohashi, and I. Tanaka, J. Chem. Phys. **107**, 2829 (1997).
[17] W. Eisfeld and K. Morokuma, J. Chem. Phys. **114**, 9430 (2001).
[18] T. A. Barckholtz and T. A. Miller, Int. Rev. Phys. Chem. **17**, 435 (1998).
[19] M. B. Pushkarsky, S. J. Zalyubovsky, and T. A. Miller, J. Chem. Phys. **112**, 10695 (2000).
[20] P. Rabinowitz, B. N. Perry, and N. Levinos, IEEE J. Quantum Electron. **22**, 797 (1986).
[21] J. E. Dennis, D. M. Gay, and R. E. Welsch, ACM Trans. Math. Softw. **7**, 369 (1981).
[22] H. M. Pickett, J. Mol. Spectrosc. **148**, 371 (1991).
[23] R. H. Judge and D. J. Clouthier, Comput. Phys. Commun. **135**, 293 (2001).
[24] J. F. Stanton (private communication).